Gauge-invariant tight-binding approach to magnetotunneling in superlattices

Daniel Paquet
Laboratoire de Bagneux, Centre National d'Etudes des Télécommunications, 196 avenue Henri Ravera, 92220 Bagneux, France
(Received 1 December 1988)

We analyze the electronic structure of a superlattice in a magnetic field parallel to the layers using a tight-binding scheme where Wannier functions centered on each well are coupled to their nearest neighbors. Gauge and translational invariances impose the condition that, within a single conduction miniband, electrons are subjected to a one-dimensional periodic potential of magnetic origin whose overall amplitude equals the miniband width. Landau levels are thus nondispersive in this energy range, and remain quasiparabolic at higher energies. The influence of interface disorder is also studied. The valence dispersion curves of a superlattice are described in an original way which leads to calculation schemes quite simpler than those already published: $\mathbf{k}\cdot\mathbf{p}$ expansion along the layers, and $\mathbf{k}$-dependent tight binding along the growth axis. The allowed energies when a transverse magnetic field is applied are then computed, with particular emphasis on the numerous anticrossings due to heavy- and light-hole coupling.

I. INTRODUCTION

Quite a few experiments show that, in short-period superlattices (SL's), electrons and holes are delocalized along the SL growth axis, and that their wave functions present some coherence over a distance much larger than the SL period. Although transport experiments (either electric[1] or optic[2–4]) along the growth axis give an indirect rough estimate of this coherence length, the clearest experiments, in our opinion, were performed using a magnetic field.[5,6] The idea was to apply a magnetic field parallel to the SL layers and thus force the electrons to close a cyclotron orbit while tunneling through the barriers, and to study the corresponding electronic structure. This was achieved for the first time by Belle, Maan, and Weimann[5] in an interband magnetoluminescence experiment on a $GaAs/Ga_{1-x}Al_xAs$ short-period SL: they found discrete lines corresponding to electron Landau levels whose energies lie within the energy range of the first SL miniband, and no structure at higher energy. These results were numerically understood on the basis of an envelope-function model of the conduction-state structure.[7] The net result is that, within the miniband-energy width, the Landau-level energies hardly depend on the position of the cyclotron-orbit center along the growth axis: the electron tunnel across the barriers and do not "feel" the positions of these barriers. On the contrary, at higher energies, the effect of the SL periodic-potential modulation is dominant, and the Landau levels are highly dispersive. The same type of analysis has been recently performed for hole states,[8] with similar results.

Our aim in this paper is to get a better physical insight into and a simpler treatment of this magnetotunneling effect, using a model where the SL states are derived from the single-quantum-well ones through a nearest-neighbor tight-binding scheme. In Sec. II we shall derive the electron states in the presence of a transverse magnetic field, and show that the Landau-level characteristics are a consequence of both gauge[9] and magnetic translational[10,11] invariance. Although much of the techniques used in this derivation can be found in various classical papers,[9–13] we found it useful for the sake of clarity to bring them all together in one place and to apply them carefully to our specific problem. The case of hole states, which is far more complex, will be treated in Sec. III. The valence structure of the superlattice, for a zero magnetic field, will be first described using an original scheme which mixes tight-binding and $\mathbf{k}\cdot\mathbf{p}$ formalisms. The hole states will be then defined according to the SL magnetic symmetries, and the structure of the hole Landau levels will be discussed. Our results will be summed up and briefly commented on in the conclusion.

II. SUPERLATTICE CONDUCTION STATES

Here we shall first precisely define the tight-binding description of conduction states at zero magnetic field, and then generalize it to the finite-field case.

A. The zero-field case

In absence of magnetic field the conduction states of $GaAs/Ga_{1-x}Al_xAs$ SL's are traditionally described using a Kronig-Penney model. Denote by V the conduction-band offset; L_w, the well width; L_b, the barrier width; z, the growth axis; and $\mathbf{r}_\parallel$, any vector parallel to the layers. The electrons are subjected to a periodic effective potential, which, within a period $d=L_w+L_b$, takes the form

$$V(\mathbf{r}_\parallel,z)=\begin{cases}0 & \text{if } |z|\le L_w/2\ , \quad (1a)\\ V & \text{if } L_w/2\le|z|\le d/2\ . \quad (1b)\end{cases}$$

Here, V is assumed to be positive, and the origin $z=0$ lies in the middle of a GaAs quantum well.

Assuming now that the electrons in the two compounds have the same effective mass m^*, the Kronig-Penney Hamiltonian takes the familiar form

$$H=-\frac{\hbar^2}{2m^*}\Delta_{\parallel}-\frac{\hbar^2}{2m^*}\frac{\partial^2}{\partial z^2}+V(\mathbf{r}_{\parallel},z)\ . \tag{2}$$

One easily finds the miniband energies $E^b(q)$, either by solving the Kronig-Penney equations[14] or simply by diagonalizing H when written on a plane-wave basis, and gets the dispersion curves

$$\mathcal{E}^b(\mathbf{k}_{\parallel},q)=E^b(q)+\frac{\hbar^2}{2m^*}\mathbf{k}_{\parallel}^2\ , \tag{3}$$

which are labeled by the miniband index b, the transverse wave vector $\mathbf{k}_{\parallel}$, and the longitudinal wave vector q, which ranges from $-\pi/d$ to π/d. The corresponding wave functions are the product of transverse plane waves by longitudinal Bloch waves:

$$\langle \mathbf{r}_{\parallel},z|b,\mathbf{k}_{\parallel},q\rangle=\frac{1}{(L_xL_y)^{1/2}}\exp(i\mathbf{k}_{\parallel}\cdot\mathbf{r}_{\parallel})\times\frac{1}{\sqrt{N}}\exp(iqz)\Phi_{b,q}(z)\ ,$$

where L_x and L_y are the transverse dimensions of the layer area S, Nd is the length of the sample along z, and $\Phi_{b,q}$ is a periodic function of z fulfilling the normalization condition,

$$\int_0^d\Phi^*_{b,d}(z)\Phi_{b,q}(z)dz=1\ .$$

The periodic part of the Bloch function, $\Phi_{b,q}$, is defined up to an overall phase factor. However, as the potential V is even, it can be chosen real, and fulfilling the symmetry relation $\Phi_{b,-q}(z)=\mp\Phi_{b,q}(-z)$, where the sign remains constant within a given miniband. Finally, it is unambiguously defined if one imposes that $\Phi_{b,q}(z)$ is a continuous function of q. With these prescriptions, let us now define longitudinal Wannier wave functions as

$$W_{b,n}(z)=\frac{1}{\sqrt{N}}\sum_q\exp[iq(z-nd)]\Phi_{b,q}(z)\ .$$

One evidently gets $W_{b,n}(z)=w_{b,0}(z-nd)$, and one can easily show that, with these definitions, the Wannier functions are localized[15] in each well, have a given parity relative to the center of the well, are orthogonal to each other, and are very similar to single-quantum-well eigenstates (for an example, see the hole case in Sec. III). We now choose the generalized Wannier orthogonal basis $|b,\mathbf{k}_{\parallel},n\rangle$ for the conduction states:

$$\langle \mathbf{r}_{\parallel},z|b,\mathbf{k}_{\parallel},n\rangle=\frac{1}{\sqrt{S}}\exp(i\mathbf{k}_{\parallel}\cdot\mathbf{r}_{\parallel})w_{b,n}(z)\ .$$

In this basis the conduction Hamiltonian takes a tight binding form

$$\langle b_1,\mathbf{k}_{\parallel,1},n_1|H|b_2,\mathbf{k}_{\parallel,2},n_2\rangle=\delta_{b_1,b_2}\delta_{\mathbf{k}_{\parallel,1},\mathbf{k}_{\parallel,2}}\left[\frac{\hbar^2\mathbf{k}_{\parallel,1}^2}{2m^*}\delta_{n_1,n_2}+t^{b_1}_{|n_2-n_1|}\right]\ ,$$

where the hopping integrals

$$t^b_{|n|}=(1/N)\sum_q\cos(qnd)E^b(q)$$

are real. As shown by Bastard,[16] the dispersion curves along z are extremely well fitted by the approximation $E^b(q)=t^b_0+2t^b_{|1|}\cos(qd)$, and the conduction states are thus modeled by the nearest-neighbor tight-binding Hamiltonian

$$H=\sum_{b,\mathbf{k}_{\parallel},n}\left[|b,\mathbf{k}_{\parallel},n\rangle\left[\frac{\hbar^2\mathbf{k}_{\parallel}^2}{2m^*}+t^b_0\right]\langle b,\mathbf{k}_{\parallel}n|+|b,\mathbf{k}_{\parallel},n\rangle t^b_{|1|}\langle b,\mathbf{k}_{\parallel},n+1|+\text{c.c.}\right]\ , \tag{4}$$

where $t^b_{|1|}$ can be understood as the tunneling integral between two successive single-quantum-well states. After performing a Fourier transform along the transverse direction, this Hamiltonian takes the simple form

$$H=\sum_{b,n}\int_S d^3r_{\parallel}\left[|b,\mathbf{r}_{\parallel},n\rangle\left[\frac{-\hbar^2}{2m^*}\Delta_{\parallel}+t^b_0\right]\langle b,\mathbf{r}_{\parallel},n|+|b,\mathbf{r}_{\parallel},n\rangle t^b_{|1|}\langle b,\mathbf{r}_{\parallel},n+1|+\text{c.c.}\right]\ , \tag{5}$$

where the bands are clearly decoupled.

B. Gauge invariance

The standard gauge principle implies that physics is unchanged when the wave functions are multiplied by a *position-dependent phase factor* $\chi(\mathbf{r}_{\parallel},z)$. Denoting U this unitary transform, the electron charge being $-e$,

$$U=\int d^2r_{\parallel}\int dz\ |\mathbf{r}_{\parallel},z\rangle\exp\left[i\frac{e}{\hbar}\chi(\mathbf{r}_{\parallel},z)\right]\langle \mathbf{r}_{\parallel},z|\ , \tag{6}$$

the transformed Hamiltonian $H'=U^{\dagger}HU$ is obtained from (2) by the standard substitution $-i\hbar\nabla\rightarrow-i\hbar\nabla+e\,\mathbf{A}$, where $\mathbf{A}(\mathbf{r}_{\parallel},z)=\nabla\chi$ is the vector potential. This transformation appears more difficult to perform directly on Eq. (5). However, as the Wannier functions are localized and orthogonal, we choose a discrete approximation of U (Ref. 9) as

$$\tilde{U}=\sum_{b,n}\int_S d^2r_{\parallel}\ |b,\mathbf{r}_{\parallel},n\rangle\exp\left[i\frac{e}{\hbar}\chi(\mathbf{r}_{\parallel},nd)\right]\langle b,\mathbf{r}_{\parallel},n|\ , \tag{7}$$

which has the virtue of remaining unitary while not mixing the band indices. This approximation is clearly valid as long as χ varies slowly on the scale of the period. The gauge-transformed version of (5), reduced to a single band b, becomes

$$H_b=\sum_n \int_S d^2r_\parallel \left[|\mathbf{r}_\parallel n,\rangle \left\{ \frac{[-i\hbar\nabla+e\,\mathbf{A}_\parallel(\mathbf{r}_\parallel,nd)]^2}{2m^*}+t_0 \right\} \langle \mathbf{r}_\parallel,n| \right.$$
$$\left. +|\mathbf{r}_\parallel,n\rangle t_1 \exp\left[-i\frac{e}{\hbar} d A_z(\mathbf{r}_\parallel,(n+\tfrac{1}{2})d) \right] \langle \mathbf{r}_\parallel,n+1| + \text{c.c.} \right] . \tag{8}$$

Thus the gauge transform introduces phase factors in the hopping term. Applying now the minimal coupling principle,[17] *we shall assume (8) to be valid even when the magnetic field* $\mathbf{B}$ *is nonzero;* that is, when $\mathbf{A}$ is not a gradient. Note that the approximation of (6) by (7) drops any interband coupling due to the magnetic field.[12] It is actually a coarse-grained approximation where the averaging length is of the order of the Wannier functions' extent, i.e., at least the well width L_w. Consequently, local effects like single-quantum-well diamagnetic shifts[18,19] and interface effects[20] are totally neglected.

C. Magnetic translational invariance

In the case we shall discuss, where the magnetic field is homogeneous, physics must remain unchanged when translating the gauge origin:

$$\mathbf{A}'(\mathbf{r}_\parallel,z)=\mathbf{A}(\mathbf{r}_\parallel-\mathbf{R}_\parallel,z-pd) .$$

This corresponds to the gauge change

$$\mathbf{A}'(\mathbf{r}_\parallel,z)=\mathbf{A}(\mathbf{r}_\parallel,z)+\nabla\chi_{\mathbf{R}_\parallel,p}(\mathbf{r}_\parallel,z) . \tag{9}$$

Let us define the magnetic translation operator as the product of the geometric translation by the gauge:[10,11]

$$\Pi_{\mathbf{R}_\parallel,p}=\int_S d^2r_\parallel \sum_n |\mathbf{r}_\parallel,n\rangle \exp\left[i\frac{e}{\hbar}\chi_{\mathbf{R}_\parallel,p}(\mathbf{r}_\parallel,nd) \right] \times\langle \mathbf{r}_\parallel-\mathbf{R}_\parallel,n-p| . \tag{10}$$

Both gauge and translational invariances require that the Hamiltonian commutes with all the magnetic translation operators. These operators, however, do not form a group, and do not commute with each other, due to the gauge phase factor. Let us compute the commutator:

$$[\Pi_{\mathbf{R}_\parallel,0},\Pi_{0_\parallel,1}]=\int_S d^2r_\parallel \sum_n |\mathbf{r}_\parallel,n\rangle C_{\mathbf{r}_\parallel,n}\langle \mathbf{r}_\parallel-\mathbf{R}_\parallel,n-1| ,$$

where

$$C_{\mathbf{r}_\parallel,n}=\exp\left[i\frac{e}{\hbar}[\chi_{\mathbf{R}_\parallel,0}(\mathbf{r}_\parallel,nd)+\chi_{0_\parallel,1}(\mathbf{r}_\parallel-\mathbf{R}_\parallel,nd)] \right] - \exp\left[i\frac{e}{\hbar}[\chi_{0_\parallel,1}(\mathbf{r}_\parallel,nd)+\chi_{\mathbf{R}_\parallel,0}(\mathbf{r}_\parallel,nd-d)] \right] .$$

This generic matrix element vanishes provided the two phase factors are equal; that is, if

$$\exp\left[i\frac{e}{\hbar}\int_{nd}^{(n-1)d}\frac{\partial}{\partial z}\chi_{\mathbf{R}_\parallel,0}(\mathbf{r}_\parallel,z)dz \right] = \exp\left[i\frac{e}{\hbar}\int_{\mathbf{r}_\parallel}^{\mathbf{r}_\parallel-\mathbf{R}_\parallel}\nabla_\parallel\chi_{0_\parallel,1}(\boldsymbol{\rho}_\parallel,nd)d\boldsymbol{\rho}_\parallel \right] ,$$

or, using (9), if the magnetic flux through the oriented plaquette defined by the four vertices $(\mathbf{r}_\parallel,nd)$, $(\mathbf{r}_\parallel-\mathbf{R}_\parallel,nd)$, $(\mathbf{r}_\parallel-\mathbf{R}_\parallel,nd-d)$, $(\mathbf{r}_\parallel,nd-d)$ is an integer multiple of the flux quantum $\Phi_0=h/e$. Consequently, assuming the magnetic field $\mathbf{B}$ is parallel to the x axis, we find that the magnetic translations form a commutative group if the translations along y (perpendicular to the growth axis and to $\mathbf{B}$) are integer multiples of the length $R_0=2\pi a_0^2/d$, where a_0 is the magnetic length $a_0=(\hbar/eB)^{1/2}$. *The presence of the magnetic field, due to flux quantization, induces a new periodicity along the y axis.*

One can now construct a symmetry-adapted orthogonal basis:

$$|k_x,K_y,q,s\rangle=\frac{1}{\sqrt{NM}}\sum_{n,m}\exp(iK_y mR_0+iqnd)\Pi_{0,mR_0,nd}|k_x,K_y+2s\pi/R_0,n=0\rangle , \tag{11}$$

where MR_0 is the SL spatial extent along y, s any integer, and K_y a new magnetic wave vector along y, whose length is limited to the first magnetic Brillouin zone

$$[-\pi/R_0,\pi/R_0]\equiv[-d/2a_0^2,d/2a_0^2] .$$

From the commutation of H with the whole magnetic group, we deduce that H is diagonal in k_x, K_y, and q, and mixes only the s quantum numbers.

D. Energy spectrum

Let us now specialize to the Landau gauge parallel to the growth axis: $A=(0,0,By)$. The single-band Hamiltonian (8) takes the simple form

$$H_b=\sum_n \int_S d^2r_\parallel \left[|\mathbf{r}_\parallel,n\rangle \left\{ \frac{-\hbar^2}{2m^*}\Delta_\parallel+t_0 \right\} \langle \mathbf{r}_\parallel,n| + |\mathbf{r}_\parallel,n\rangle t_{|1|} \exp\left[-i\frac{yd}{a_0^2} \right] \langle \mathbf{r}_\parallel,n+1| + \text{c.c.} \right] , \tag{12}$$

and the magnetic Bloch states may be written, using (8)–(11), as

$$|k_x,K_y,q;s\rangle=\left[\frac{M}{NS}\right]^{1/2}\int_S dx\,dy\sum_n \exp\left[iqnd+ik_x x+i\left[K_y-\frac{d}{a_0^2}s\right]y\right]|x,y,n\rangle\ ,$$

where s is any integer; that is, comparing with the eigenstates at zero field:

$$|k_x,K_y,q;s\rangle=|k_x,K_y+sd/a_0^2,q\rangle\ ,$$

where the plane wave along y is now normalized to the magnetic unit cell. In this basis, the matrix elements of the Hamiltonian (12) take the simple form

$$\langle k_x,K_y,q;s_1|H_b|k_x,K_y,q;s_2\rangle=\left\{t_0+\frac{\hbar^2}{2m^*}\left[\left[K_y+s_1\frac{d}{a_0^2}\right]^2+k_x^2\right]\right\}\delta_{s_1,s_2}+t_{|1|}[\exp(iqd)\delta_{s_2,s_1+1}+\exp(-iqd)\delta_{s_2,s_1-1}]\ , \tag{13}$$

which, after a Fourier transform along y, becomes

$$H_b=\int dy\int dk_x\sum_q|k_x,y,q\rangle\left[t_0+\frac{\hbar^2}{2m^*}\left[k_x^2-\frac{\partial^2}{\partial y^2}\right]+2t_{|1|}\cos\left[\frac{d}{a_0^2}y-qd\right]\right]\langle k_x,y,q|\ . \tag{14}$$

One sees that *the energy does not depend on the longitudinal wave vector q* and that the motion along y is described by the *Mathieu* equation (one-dimensional motion in a cosine potential). The form of the dispersion relations is then obvious.

(i) No dispersion along the growth axis z.

(ii) Normal kinetic energy along the magnetic field axis x.

(iii) Concerning the motion along the third direction y, (a) bound quasinondispersive states for energies between $-2t_{|1|}$ and $+2t_{|1|}$ that are within the original miniband width, and (b) scattering states at higher energies, with small gaps at $K_y=0$ and $\mp d/2a_0^2$ and an energy essentially equal to the normal kinetic one.

This agrees with the main results obtained experimentally[5] and numerically.[7] To get a quantitative analysis, let us define the quantities $Y=yd/a_0^2$, $\hbar\omega_c=eBd(W/2m^*)^{1/2}$, which is the small-field cyclotron frequency, and $W=-4t_{|1|}$, which is the miniband width. If we define the energy origin as the bottom of the miniband, the Mathieu equation becomes, in reduced units,

$$\left[-\left[\frac{\hbar\omega_c}{W}\right]^2\frac{\partial^2}{\partial Y^2}-\tfrac{1}{2}\cos Y\right]\Psi=\left[\frac{E}{W}-\frac{1}{2}\right]\Psi\ .$$

We plot in Fig. 1 the Landau-level energies and bandwidths as a function of the magnetic field in these reduced units. One sees on this fan diagram that, at low field, the energies scale on the magnetic field and that the level becomes dispersive for energies of the order of the miniband width. However, for high fields, even the first level becomes dispersive. The crossover corresponds to $W\simeq(\hbar^2/2m^*)(d^2/a_0^4)$; that is, to the case where the magnetic length becomes of the order of magnitude of the period, a point where our discrete approximation of the gauge transform breaks down.

We should like to underline two important points.

The magnetic coupling between different minibands is not taken into account, due to the discrete form of the gauge transforms $\tilde{U}$ [see Eq. (7)].

The lack of dispersion along the growth axis is not an artifact of the nearest-neighbor approximation. Had we taken all of the couplings derived from the exact miniband dispersion relation $E^b(q)$, the same derivation would have led to a Hamiltonian similar to (14):

$$H_b=\int dy\,dk_x\sum_q|k_x,y,q\rangle\left[\frac{\hbar^2}{2m^*}\left[k_x^2-\frac{\partial^2}{\partial y^2}\right]+E^b\left[q-\frac{1}{a_0^2}y\right]\right]\langle k_x,y,q|\ ,$$

which is simply obtained from the single-band dispersion curve (3) by the substitution[12,13]

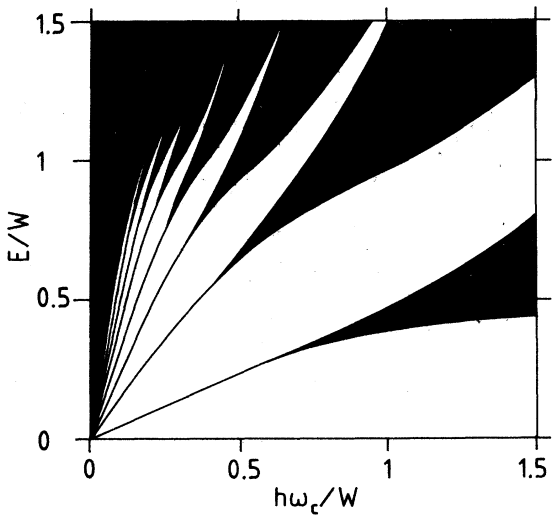

FIG. 1. Allowed energies (in black) for $k_x=0$ as a function of the transverse magnetic field for a single conduction miniband. The energy and magnetic field are in reduced units.

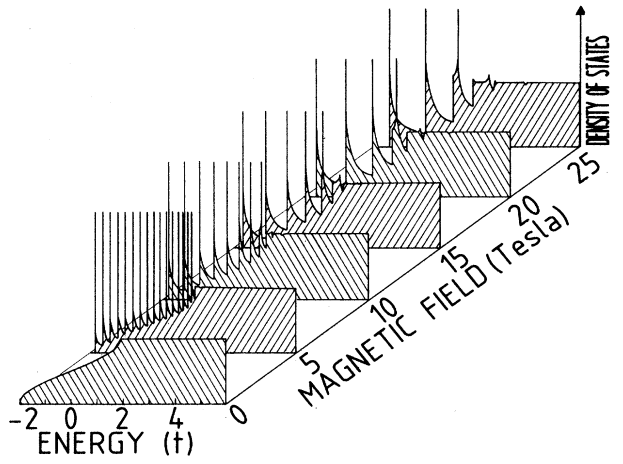

FIG. 2. Conduction density of states for different values of the magnetic field.

$$(\mathbf{k}_{\parallel},q)\rightarrow(k_x,-i(\partial/\partial y),q-e\hbar^{-1}A_z)\ . \tag{15}$$

The effective potential along y is again periodic with period R_0, and the conclusions (i)–(iii) remain valid.

As a consequence of the particular form of H_b, the density of states (DOS) displays, within the miniband width, a series of one-dimensional singularities corresponding to Landau levels. The DOS remains essentially constant at higher energies (two-dimensional dispersion curves along x and y) with small accidents due to tiny gaps at the center edges of the magnetic Brillouin zone. These results are illustrated in Fig. 2, where the conduction DOS is plotted at various magnetic fields for the sample studied in Ref. 5 (miniband $4t_{|1|}=116$ meV, period $d=50.4$ Å, $m^*=0.078m_0$).

E. Eigenstates

Although the Landau energies do not depend on the quantum number q, the corresponding eigenfunctions are q dependent. Using the Bloch theorem, the eigenfunctions of Eq. (14) can be labeled $|k_x,K_y,q;\ell\rangle$, where ℓ is the Landau-level index, with

$$\langle x,y,n\,|k_x,K_y,q;\ell\rangle=\frac{1}{(MNL_x)^{1/2}}M_{\ell,K_y}(y-qa_0^2)\times\exp\left[i(k_xx+K_yy+qnd)\right],$$

and where the Mathieu functions M_{ℓ,K_x} are periodic and normalized on the period R_0. One can then define magnetic Wannier functions in the y-z plane as

$$|k_x,m,n;\ell\rangle=\frac{1}{\sqrt{NM}}\sum_{K_y,q}\exp(-iK_ymR_0-iqnd)|k_x,K_y,q;\ell\rangle\ .$$

One gets

$$\langle k_x,y,n_1|k_x,m,n;\ell\rangle=\exp\left[iy(n_1-n)\frac{2\pi}{R_0}\right]\times\frac{1}{M}\sum_{K_y}\exp[iK_y(y-mR_0)]\times\hat{M}_{\ell,K_y}(n_1-n)\ ,$$

where

$$\hat{M}_{\ell,K_y}(s)=\frac{1}{R_0}\int_0^{R_0}e^{-i(2\pi/R_0)sy}M_{\ell,K_y}(y)dy$$

is the Fourier transform of the periodic Mathieu function. In this magnetic Wannier basis, the Hamiltonian takes the new tight-binding form:

$$H=\int dk_x\sum_{m_1,m_2,n,\ell}|k_x,m_1,n;\ell\rangle\times\left[\frac{\hbar^2k_x^2}{2m^*}+\tau^{\ell}_{m_1-m_2}\right]\langle k_x,m_2,n;\ell|\ ,$$

with

$$\tau^{\ell}_s=\frac{1}{M}\sum_K E_{\ell}(K_y)e^{iK_yR_0s}\ .$$

This means that, due to the lack of q dispersion, Wannier states with different n indices are uncoupled. Furthermore, the low-ℓ Landau levels are quasinondispersive; this implies that the corresponding couplings constants τ^{ℓ}_s are vanishing for $s\neq0$, and that the magnetic Wannier states can be considered as localized eigenstates. In the latter case, for the first Landau level, the Mathieu wave functions can be approximately computed, by modeling the cosine potential as a periodic array of parabolic wells. One then finds the energy $E_1(K_y)=\hbar\omega_c/2$, and the localized eigenstates,

$$\langle k_x,y,n_1|k_x,m,n;\ell=1\rangle\sim\exp\left[iy(n_1-n)\frac{2\pi}{R_0}\right]\times\frac{\sin(\pi y/R_0)}{y-mR_0}\times\exp\left[-(n_1-n)^2\frac{\hbar\omega_c}{W}\right]\ .$$

This means that, in the first Landau level, the electrons tunnel through the barriers, and that the cyclotron orbit embraces $(2W/\hbar\omega_c)^{1/2}$ successive quantum wells.

Let us now discuss the high-energy Landau eigenstates. In that case the solution of the Mathieu equation is straightforward. The kinetic energy is dominant as compared with the cosine potential one. We thus get

$$E_{\ell}(K_y)=\frac{\hbar^2K_y^2}{2m^*}\quad\text{and}\quad M_{\ell K_y}(y)=\frac{\exp[i\ell(2\pi y/R_0)]}{(R_0)^{1/2}}\ ,$$

which leads to the following form of the magnetic Wannier states:

$$\langle k_x,y,n_1|k_x,m,n;\ell\rangle=\delta_{n_1,n+\ell}\times\exp\left[i\ell\frac{2\pi y}{R_0}\right]\frac{\sin(\pi y/R_0)}{y-mR_0}\ .$$

This means that the dispersive Landau levels (at energies higher than the miniband maximum) remain essentially localized in a single quantum well: there is no tunneling along the SL growth direction.

F. Influence of disorder

Let us assume now that there exists some randomness in the confinement energy of the quantum wells, due, for instance, to fluctuations in the quantum-well width. This is roughly modeled by adding a random potential

$$V=\sum_{\mathbf{k}_\parallel,n}|\mathbf{k}_\parallel,n\rangle\delta V_n\langle\mathbf{k}_\parallel,n|\ ,$$

where the δV_n are independent random variables with a vanishing average and a common mean square root σ_V. This potential clearly neglects the interface roughness (disorder in the transverse direction), whose effect is rather difficult to account for.[21] Adding this random potential clearly breaks the translational symmetry along z, and thus the magnetic periodicity along y. However, averaging over the disorder will restore these symmetries. We thus assume that the average electron propagator takes the form

$$G(z)=\sum_{k_z,K_y,q,\ell}|k_x,K_y,q;\ell\rangle\frac{1}{z-\frac{\hbar^2k_x^2}{2m^*}-E_\ell(K_y)-\Sigma_{k_x,K_y,\ell}(z)}\langle k_x,K_y,q;\ell|\ ,$$

where we introduced a self-energy Σ which we shall estimate using second-order renormalized perturbation theory:

$$\Sigma_{k_x,K_y,\ell}(z)=\overline{\langle k_x,K_y,q;\ell|V+VG(z)V|k_x,K_y,q;\ell\rangle}\ ,$$

where the overbar denotes averaging. Noting that the random potential can be rewritten in the magnetic eigenbasis as

$$V=\sum_{\substack{q_1,q_2,\ell_1,\ell_2\\k_x,K_y,s,n}}|k_x,K_y,q_1;\ell_1\rangle\delta V_n e^{i(n-s)(q_1-q_2)d}\hat{M}_{\ell_1}(s)\hat{M}^*_{\ell_2}(s)\langle k_x,K_y,q_2;\ell_2|\ ,$$

and using the orthogonality of the Mathieu functions, one gets the miraculously simple result

$$\Sigma_{k_x,k_y,\ell}(z)=\sigma_V^2\frac{1}{z-\hbar^2k_x^2/2m^*-E_\ell(K_y)-\Sigma_{k_x,K_y,\ell}(z)}\ .$$

Each level is broadened with a semielliptic shape of total width $4\sigma_V$. The average propagator takes the form

$$G(z)=\sum_{k_x,K_y,q,\ell}|k_xK_y,q,\ell\rangle\frac{1}{2\sigma_V^2}\left\{z-E_\ell(K_y)-\frac{\hbar^2k_x^2}{2m^*}-\left[\left[z-E_\ell(K_y)-\frac{\hbar^2k_x^2}{2m^*}\right]^2-4\sigma_V^2\right]^{1/2}\right\}\langle k_x,K_y,q,\ell|\ ,$$

and the imaginary part of its trace provides the average density of states. To account for the disappearance of the Landau structures at fields lower than 5 T in the sample studied,[5] we draw in Fig. 3 the average DOS at $B=5$ T for different values of the random-potential rms σ_V. The Landau-level structure is washed out around $\sigma_V/t_{|1|}=0.1$; that is, for $\sigma_V=2.9$ meV, which corresponds to fluctuations of the well width roughly amounting to one-half atomic monolayer. Furthermore, this value of the magnetic field leads to $\hbar\omega_c/W\sim8\times10^{-2}$; that is, to a ground-state wave function which extends over at least five successive quantum wells. This provides a lower bound for the coherence length. Another estimate of this quantity can be derived from the number of different Landau levels experimentally observed:[5,7] The seven observed excited states are orthogonal to each other and to the ground states, a fact which imposes on the latter to remain coherent over eight successive quantum wells. Thus the experiment gives altogether an estimate

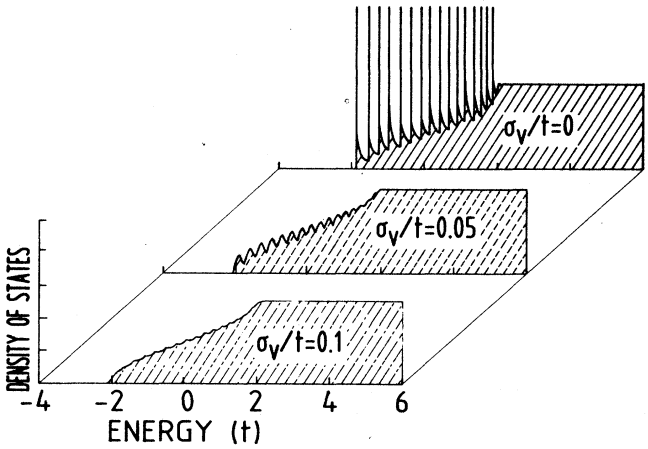

FIG. 3. Conduction density of states at a magnetic field $B=5$ T, for different values of the random-potential root mean square.

of the quality of the sample and of the coherence length along the growth axis.

III. SUPERLATTICE VALENCE STATES

We shall use the same approach as before to compute the SL valence eigenstates; namely, first build up a tight-binding Hamiltonian of the valence states in absence of magnetic field and, second, work out the spectrum at a finite transverse magnetic field, by applying at length, translational and gauge invariance.

A. The zero-field case

Neglecting the inversion asymmetry splitting, and assuming the two bulk materials to have the same effective mass, the envelope-function effective Hamiltonian for the first four valence states takes the form derived from the Luttinger[22] Hamiltonian:

$$H_{\Gamma_8}=\begin{bmatrix} H_h & C & b & 0 \\ C^* & H_l & 0 & b \\ b^* & 0 & H_l & -c \\ 0 & b^* & -c^* & H_h \end{bmatrix} .$$

This matrix operator is written in the ordered basis

$$\{\varphi_m(z)e^{i\mathbf{k}_\parallel\mathbf{r}_\parallel}|\tfrac{3}{2};m\rangle\}_{m=3/2,\,1/2,\,-1/2,\,-3/2} .$$

In the axial approximation,[23] which neglects the band warping in the x-y plane, the matrix elements are

$$H_h=\frac{\hbar^2}{2m_0}(\gamma_1-2\gamma_2)\frac{\partial^2}{\partial z^2}+V(z)-\frac{\hbar^2\mathbf{k}_\parallel^2}{2m_0}(\gamma_1+\gamma_2) ,$$

$$H_l=\frac{\hbar^2}{2m_0}(\gamma_1+2\gamma_2)\frac{\partial^2}{\partial z^2}+V(z)-\frac{\hbar^2\mathbf{k}_\parallel^2}{2m_0}(\gamma_1-\gamma_2) ,$$

$$b=\frac{\sqrt{3}}{4}\frac{\hbar^2}{m_0}(\gamma_2+\gamma_3)(k_x-ik_y)^2 ,$$

$$c=-i\sqrt{3}\frac{\hbar^2}{m_0}\gamma_3(k_x-ik_y)\frac{\partial}{\partial z} ,$$

where $V(z)$ is the effective valence potential profile, and the γ's are the Luttinger parameters, which we assume to be identical in the two materials. The off-diagonal terms in H_{Γ_8} vanish for $\mathbf{k}_\parallel=\mathbf{0}$, and the problem reduces to solving two independent Kronig-Penney problems: H_h for heavy holes and H_l for light holes. Let us now define, as we did for conduction states, heavy- and light-hole longitudinal Wannier functions $W_{h,b}(z)$ and $W_{l,b}(z)$, centered on the zeroth well. Here, b is the miniband index. For describing the valence states in the sample studied in Ref. 5, we used $\gamma_1=6.85$, $\gamma_2=2.1$, $\gamma_3=2.9$, and a valence-band offset $\Delta E_v=192$ meV. One then finds, within the well energy, three minibands: a first heavy-hole band h_1 with a rather small width ($4t_{h_1}=16$ meV), and two broader overlapping bands, a light-hole one ($4t_l=130$ meV) and a second heavy-hole one ($4t_{h_2}=-64$ meV). The associated Wannier functions are drawn in Fig. 4. They are essentially localized into a given well with a given parity, and spread only to the two adjacent wells. This justifies modeling the Kronig-Penney Hamiltonian by a nearest-neighbor tight-binding one. When the wave vector parallel to the layers is nonvanishing, we shall assume that the SL eigenstates remain linear combination of products of longitudinal Wannier states by transverse plane waves. In other words, we shall expand the SL eigenstates in the basis

$$\left.\begin{array}{l} W_{h_1}(z-nd)|\frac{3}{2},\frac{3}{2}\rangle \\ W_l(z-nd)|\frac{3}{2},-\frac{1}{2}\rangle \\ W_{h_2}(z-nd)|\frac{3}{2},-\frac{3}{2}\rangle \\ W_{h_1}(z-nd)|\frac{3}{2},-\frac{3}{2}\rangle \\ W_l(z-nd)|\frac{3}{2},-\frac{1}{2}\rangle \\ W_{h_2}(z-nd)|\frac{3}{2},\frac{3}{2}\rangle \end{array}\right\}\times\frac{1}{(L_xL_y)^{1/2}}e^{i\mathbf{k}_\parallel\cdot\mathbf{r}_\parallel} , \tag{16}$$

where n labels the quantum-well position. In this approximation we neglect the effects of the scattering states (SL bands at energies smaller than $-\Delta E_v$). Applying H_{Γ_8} on this basis will generate intrawell couplings, similar to the "mini-$\mathbf{k}\cdot\mathbf{p}$" expansion already used to describe single-quantum-well valence states,[24,14] and nearest-neighbor $\mathbf{k}_\parallel$-dependent tight-binding couplings. Denoting P_n the projection on the nth quantum-well basis, the SL Hamiltonian takes the form

$$H_{\mathrm{SL}}=\sum_{\mathbf{k}_\parallel,n}P_nH_0(\mathbf{k}_\parallel)P_n+P_{n-1}\overleftarrow{T}(\mathbf{k}_\parallel)P_n+P_{n+1}\overrightarrow{T}(\mathbf{k}_\parallel)P_n , \tag{17}$$

where $H_0(\mathbf{k}_\parallel)$, $\overleftarrow{T}(\mathbf{k}_\parallel)$, and $\overrightarrow{T}(\mathbf{k}_\parallel)$ are 6×6 matrices:

$$H_0(\mathbf{k}_\parallel)=\begin{bmatrix} E_{h_1}-\gamma_hk^2 & \gamma k_-^2s & 0 & 0 & 0 & 0 \\ \gamma k_+^2s & E_l-\gamma_lk^2 & i\tilde{\gamma}k_-p & 0 & 0 & 0 \\ 0 & -i\tilde{\gamma}k_+p & E_{h_2}-\gamma_hk^2 & 0 & 0 & 0 \\ 0 & 0 & 0 & E_{h_1}-\gamma_hk^2 & \gamma k_+^2s & 0 \\ 0 & 0 & 0 & \gamma k_-^2s & E_l-\gamma_lk^2 & -i\tilde{\gamma}k_+p \\ 0 & 0 & 0 & 0 & i\tilde{\gamma}k_-p & E_{h_2}-\gamma_hk^2 \end{bmatrix} , \tag{18}$$

$$\overleftarrow{T}(\mathbf{k}_\parallel)=\begin{bmatrix} t_{h_1} & \gamma k_-^2 s_1 & 0 & 0 & -i\tilde{\gamma}k_- s_1 & 0 \\ \gamma k_+^2 s_1 & t_l & -i\tilde{\gamma}k_- p_2 & -i\tilde{\gamma}k_- p_1 & 0 & -\gamma k_+^2 s_2 \\ 0 & i\tilde{\gamma}k_+ p_2 & t_{h_2} & 0 & \gamma k_+^2 s_2 & 0 \\ 0 & i\tilde{\gamma}k_+ p_1 & 0 & t_{h_1} & \gamma k_+^2 s_1 & 0 \\ -i\tilde{\gamma}k_+ p_1 & 0 & -\gamma k_-^2 s_2 & \gamma k_-^2 s_1 & t_l & i\tilde{\gamma}k_+ p_2 \\ 0 & \gamma k_-^2 s_2 & 0 & 0 & -i\tilde{\gamma}k_- p_2 & t_{h_2} \end{bmatrix}, \tag{19}$$

$$\overrightarrow{T}(\mathbf{k}_\parallel)=\overleftarrow{T}^\dagger(\mathbf{k}_\parallel), \tag{20}$$

with the notations

$$k_+=k_x+ik_y,\quad k_-=k_x-ik_y,$$

$$\gamma_h=(\hbar^2/2m_0)(\gamma_1+\gamma_2),\quad \gamma_1=(\hbar^2/2m_0)(\gamma_1-\gamma_2),$$

$$\gamma=(\hbar^2/2m_0)\sqrt{3/2}(\gamma_2+\gamma_3),\quad \tilde{\gamma}=(\hbar^2/2m_0)\sqrt{3}\gamma_3,$$

$$s=\langle W_{h_1}(z)|W_1(z)\rangle,\quad s_1=\langle W_{h_1}(z)|W_l(z-d)\rangle,\quad s_2=\langle W_{h_2}(z)|W_l(z-d)\rangle,$$

$$p=\left\langle W_l(z)\left|\frac{\partial}{\partial z}\right|W_{h_2}(z)\right\rangle,\quad p_1=\left\langle W_{h_1}(z)\left|\frac{\partial}{\partial z}\right|W_l(z-d)\right\rangle,\quad p_2=\left\langle W_{h_2}(z)\left|\frac{\partial}{\partial z}\right|W_l(z-d)\right\rangle.$$

The parity of the Wannier functions has been used repetitively when writing down the form of the 6×6 matrices. The matrix elements between Wannier functions are easily computed. We found, in our specific cases, the following.

Wave-function overlaps: $s=0.97$, $s_1=4\times10^{-3}$, $s_2=0.12$.
Momentum matrix elements (in units of $2\pi/d$): $p=0.20$, $p_1=0.12$, $p_2=0.08$.

Translational invariance along the growth axis implies that the q-dependent projector $P_q=(1/\sqrt{N})\sum_n e^{iqnd}P_n$ commutes with H_{SL}. The dispersion curves are thus obtained through diagonalization of the 6×6 matrix,

$$P_q H_{\mathrm{SL}} P_q=\begin{bmatrix} A & B \\ B^\dagger & A^* \end{bmatrix},$$

with

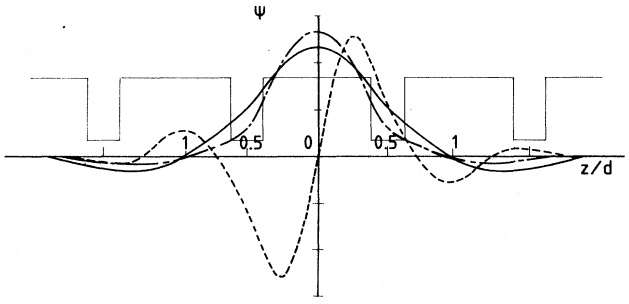

FIG. 4. Valence Wannier wave functions in the superlattice studied in Ref. 5. Dotted-dashed line, first heavy-hole miniband; solid line, light-hole miniband; dashed line, second heavy-hole miniband. The conduction-band profile is also drawn in arbitrary units, as a guide to the eyes.

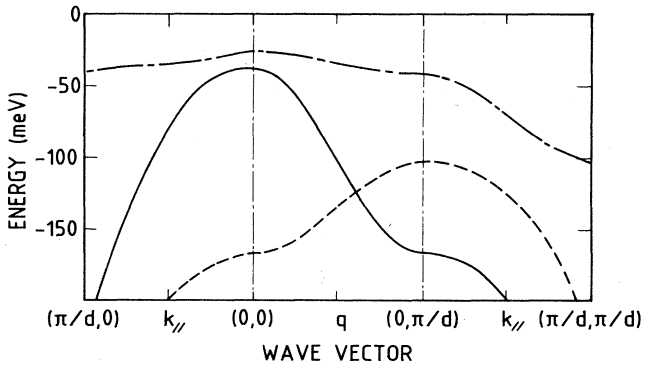

FIG. 5. Valence-subband dispersion curves for the superlattice studied in Ref. 5, whose associated Wannier wave functions are drawn in Fig. 4.

$$A=\begin{bmatrix} E_{h_1}-\gamma_h k^2+2t_{h_1}\cos(qd) & \gamma k_-^2[s+2s_1\cos(qd)] & 0 \\ \gamma k_+^2[s+2s_1\cos(qd)] & E_l-\gamma_l k^2+2t_l\cos(qd) & i\tilde{\gamma}k_-[p-2p_2\cos(qd)] \\ 0 & -i\tilde{\gamma}k_+[p-2p_2\cos(qd)] & E_{h_2}-\gamma_h k^2+2t_{h_2}\cos(qd) \end{bmatrix},$$

$$B=\begin{bmatrix} 0 & 2\tilde{\gamma}k_-p_1\sin(qd) & 0 \\ -2\tilde{\gamma}k_-p_1\sin(qd) & 0 & -2i\gamma k_+^2 s_2\sin(qd) \\ 0 & 2i\gamma k_+^2 s_2\sin(qd) & 0 \end{bmatrix}.$$

Due to the axial approximation, the dispersion curves depend only on the modulus of $\mathbf{k}_\parallel$, and can be computed for $k_x=0$. In that case, A becomes real and B pure imaginary. Furthermore, time-reversal (Kramers) invariance implies that the eigenvalues are twice degenerate. They are easily found by diagonalizing the 3×3 matrix $A+B$. The resulting dispersion curves for our specific case are drawn in Fig. 5.

B. Hole states in a transverse magnetic field

Before introducing a nonvanishing magnetic field, let us first study the influence of a gauge transform on the SL Hamiltonian. We choose here also a discrete form of the gauge transforms, similar to (7), but where the phase is changed into its opposite to account for the positive charge of the holes:

$$\tilde{U}=\sum_{b,n}\int_S d^2r_\parallel\,|b,\mathbf{r}_\parallel,n\rangle\exp\left[-i\frac{e}{\hbar}\chi(\mathbf{r}_\parallel,nd)\right]\langle b,\mathbf{r}_\parallel,n|\,,$$

where b is the band index, running from 1 to 6 according to the convention (16). The gauge-transformed version of (17) becomes

$$\tilde{U}^\dagger H_{\mathrm{SL}}\tilde{U}=\int_S d^2r_\parallel\sum_n P_nH_nP_n+P_{n-1}\left[\frac{\exp i\frac{e}{\hbar}dA_z(\mathbf{r}_\parallel,nd-d/2)\overleftarrow{\mathrm{T}}_n+\overleftarrow{\mathrm{T}}_{n-1}\exp\left[i\frac{e}{\hbar}dA_z(\mathbf{r}_\parallel,nd-d/2)\right]}{2}\right]P_n$$
$$+P_{n+1}\left[\frac{\exp\left[i\frac{e}{\hbar}dA_z(\mathbf{r}_\parallel,nd+d/2)\right]\overrightarrow{\mathrm{T}}_n+\overrightarrow{\mathrm{T}}_{n+1}\exp\left[i\frac{e}{\hbar}dA_z(\mathbf{r}_\parallel,nd+d/2)\right]}{2}\right]P_n\,, \tag{21}$$

where H_n, $\overleftarrow{\mathrm{T}}_n$, and $\overrightarrow{\mathrm{T}}_n$ are deduced from $H_0(\mathbf{k}_\parallel)$, $\overleftarrow{\mathrm{T}}(\mathbf{k}_\parallel)$, and $\overrightarrow{\mathrm{T}}(\mathbf{k}_\parallel)$ by substituting in (18), (19), and (20) $\mathbf{k}_\parallel$ by $-i\nabla_\parallel-(e/\hbar)\mathbf{A}_\parallel(\mathbf{r}_\parallel,nd)$. Note that the hoping terms have been symmetrized in order that the Hamiltonian remains Hermitian even if the vector potential is not a gradient. To get the SL Hamiltonian in the presence of a nonvanishing magnetic field, we must add to (21) the Zeeman term[22] $(\hbar e/m_0)\kappa\mathbf{J}\cdot\mathbf{B}\equiv\tilde{\kappa}\mathbf{J}_x\cdot\mathbf{B}$. $\mathbf{J}$ is the angular-momentum operator for spin $\frac{3}{2}$, and κ is a new Luttinger coefficient whose value for GaAs is 1.2. This extra term, written in the basis (16), generates, for a magnetic field along x, intrawell terms,

$$J_x^{\mathrm{diag}}=\begin{bmatrix} 0 & 0 & 0 & 0 & 0 & \frac{\sqrt{3}}{2}s & 0 \\ 0 & 0 & 0 & 0 & \frac{\sqrt{3}}{2}s & 1 & 0 \\ 0 & 0 & 0 & 0 & 0 & 0 & 0 \\ 0 & \frac{\sqrt{3}}{2}s & 0 & 0 & 0 & 0 & 0 \\ \frac{\sqrt{3}}{2}s & 1 & 0 & 0 & 0 & 0 & 0 \\ 0 & 0 & 0 & 0 & 0 & 0 & 0 \end{bmatrix},$$

and hopping terms,

$$\overleftarrow{J}_x=\begin{bmatrix} 0 & 0 & 0 & 0 & \frac{\sqrt{3}}{2}s_1 & 0 \\ 0 & 0 & -\frac{\sqrt{3}}{2}s_2 & -\frac{\sqrt{3}}{2}s_1 & 0 & 0 \\ 0 & \frac{\sqrt{3}}{2}s_2 & 0 & 0 & 0 & 0 \\ 0 & \frac{\sqrt{3}}{2}s_1 & 0 & 0 & 0 & 0 \\ \frac{\sqrt{3}}{2}s_1 & 0 & 0 & 0 & 0 & -\frac{\sqrt{3}}{2}s_2 \\ 0 & 0 & 0 & 0 & \frac{\sqrt{3}}{2}s_2 & 0 \end{bmatrix}, \quad \overrightarrow{J}_x=\overleftarrow{J}_x^{\dagger} .$$

Choosing again the gauge $\mathbf{A}=(0,0,By)$, taking advantage of the magnetic translation symmetry along y, and assuming $k_x=0$, we get the q-dependent magnetic Hamiltonian:

$$\tilde{H}_q(B)=\begin{bmatrix} H_q(B) & V_q(B) \\ V_q(B) & H_q(B) \end{bmatrix}, \tag{22}$$

$$H_q(B)=\begin{bmatrix} a_1 & b & 0 \\ b^{\dagger} & c & d \\ 0 & d^{\dagger} & a_2 \end{bmatrix}, \quad V_q(B)=\begin{bmatrix} 0 & e & 0 \\ e^{\dagger} & f & g \\ 0 & g^{\dagger} & 0 \end{bmatrix}$$

and

$$a_{1,2}=E_{h_{1,2}}+\gamma_h\frac{\partial^2}{\partial y^2}+2t_{h_{1,2}}\cos\left[\frac{yd}{a_0^2}+qd\right],$$

$$b=\gamma s_1\left[\frac{\partial^2}{\partial y^2}\cos\left[\frac{yd}{a_0^2}+qd\right]+\cos\left[\frac{yd}{a_0^2}+qd\right]\frac{\partial^2}{\partial y^2}\right]+\gamma s\frac{\partial^2}{\partial y^2},$$

$$c=E_l+\gamma_l\frac{\partial^2}{\partial y^2}+2t_l\cos\left[\frac{yd}{a_0^2}+qd\right],$$

$$d=-i\tilde{\gamma}p\frac{\partial}{\partial y}-i\sqrt{3}s_2\tilde{\kappa}B\sin\left[\frac{yd}{a_0^2}+qd\right]+i\tilde{\gamma}p_2\left[\frac{\partial}{\partial y}\cos\left[\frac{yd}{a_0^2}+qd\right]+\cos\left[\frac{yd}{a_0^2}+qd\right]\frac{\partial}{\partial y}\right],$$

$$e=\frac{\sqrt{3}}{2}\tilde{\kappa}sB+\sqrt{3}s_1\tilde{\kappa}B\cos\left[\frac{yd}{a_0^2}+qd\right]-\tilde{\gamma}p_1\left[\frac{\partial}{\partial y}\sin\left[\frac{yd}{a_0^2}+qd\right]+\sin\left[\frac{yd}{a_0^2}+qd\right]\frac{\partial}{\partial y}\right],$$

$$f=\tilde{\kappa}B ,$$

$$g=-i\gamma s_2\left[\frac{\partial^2}{\partial y^2}\sin\left[\frac{yd}{a_0^2}+qd\right]+\sin\left[\frac{yd}{a_0^2}+qd\right]\frac{\partial^2}{\partial y^2}\right].$$

From the particular form of $\tilde{H}_q(B)$ [Eq. (22)], one sees that the eigensystem

$$\begin{bmatrix} H_q(B) & V_q(B) \\ V_q(B) & H_q(B) \end{bmatrix}\begin{bmatrix} \varphi_1 \\ \varphi_2 \end{bmatrix}=E_q(B)\begin{bmatrix} \varphi_1 \\ \varphi_2 \end{bmatrix}$$

can be split into two independent 3×3 problems, amounting to the diagonalization of either $H_q(B)+V_q(B)$ (with $\varphi_1=\varphi_2$) or $H_q(B)-V_q(B)$ (with $\varphi_1=-\varphi_2$). Note that these two families of eigenstates interchange when B is changed into $-B$, as the first family combines states carrying the angular-momentum projections $S_x=\frac{3}{2}$ and $-\frac{1}{2}$, while the second one mixes $S_x=-\frac{3}{2}$ with $\frac{1}{2}$.

As for the conduction states, we find that the effective Hamiltonian (22) is periodic in the y direction, with the magnetic period $R_0=2\pi a_0^2/d$, and that the eigenvalues do not depend on q. The eigenstates are thus labeled by the two wave vectors q and K_y (we assumed $k_x=0$), and the 3×3 eigenproblem is easily solved by expanding the magnetic Bloch states in Fourier series. This leads to di-

agonalize an infinite block-tridiagonal matrix. This was easily performed after checking that convergence was achieved when using only 31 plane waves [from $-15(2\pi/R_0)$ to $15(2\pi/R_0)$]. The results are summarized in Fig. 6 where we draw, for $k_x=0$, the allowed energies as a function of the magnetic field. The first Landau level originates from the first heavy-hole miniband. Its energy varies quasilinearly with the magnetic field, and displays no dispersion up to 20 T. The higher Landau levels are repulsed by or anticross with levels originating from the light-hole miniband, and thus behave sublinearly with the field. Furthermore, they become dispersive as soon as their energy reaches the top of the light-hole miniband. For lower energies the hole structure is very complex, as one gets an infinite number of anticrossing between levels issued from the top of the two minibands. The point noted by a star on Fig. 6, which corresponds to a vanishing field and to the light-hole–band edge, is actually an accumulation point for anticrossings, and the allowed energies define, in its surrounding, a set which looks like a fractal. The fan diagram drawn on Fig. 6 is not symmetric, as we plotted one level family for positive fields and the other for negative fields. This asymmetry is only due to the Zeeman term, which breaks the time-reversal invariance.

Let us note that the coupling between different minibands comes only from the form of the Luttinger Hamiltonian: that is, from the SL axial symmetry; the discrete form of the gauge transforms we used still does not couple states with different symmetries. We also find here an Hamiltonian which is periodic in the y direction, with period R_0. This is again the consequence of the magnetic translational invariance. The absence of dispersion along z again implies that one can construct states localized (in the growth direction only) around a given well which remain eigenstates. Furthermore, the lack of dispersion in K_y at low fields for low-index Landau states implies that the associated magnetic Wannier functions (localized in both z and y directions) are *bona fide* eigenstates.

Our approximation, which consists of neglecting the coupling with the deeper hole-scattering states, seems to be correct, as we discussed only the Landau states which lie at least 60 meV higher than the maximum of the miniband issued from the second heavy-hole states (see Fig. 5) and 130 meV higher than the barrier bottom. However, the details of the anticrossings between high-Landau levels is so complex that they must be model dependent. Indeed, for a 19-T magnetic field, our simple calculation leads, for the first six levels, to energies which coincide, within an error of 1 meV, to the values computed by Fasolino and Altarelli,[25] who solved numerically the exact Luttinger Hamiltonian for the same superlattice using rather heavy finite-difference techniques, although our estimation quantitatively differs from their results in the anticrossing region. Finally, let us note that, due to these numerous anticrossings, the index of the Landau levels no longer labels the numbers of zeros in the wave functions. The approximate selection rules commonly used for optical transitions (same Landau-level index for the involved valence and conduction states) are thus no longer valid.

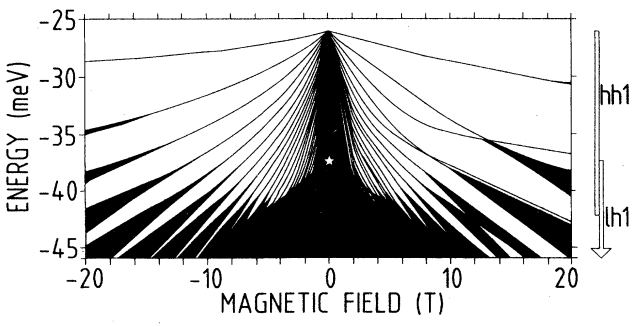

FIG. 6. Allowed energies (in black) for $k_x=0$ as a function of the transverse magnetic field, for the valence states of the superlattice studied in Ref. 5. The star points out the edge of the first light-hole (lh_1) miniband, which partially overlaps the first heavy-hole (hh_1) miniband.

IV. CONCLUSION

The main result of this paper was to show that both gauge and translational invariance impose that, within a single miniband, electrons in a superlattice with a transverse magnetic field "feel" a one-dimensional periodic potential whose overall amplitude is equal to the miniband width. This simple result explains why nondispersive Landau levels exist only within the miniband-energy range. Due to the high degeneracy of these states, many different representations of the eigenstates can be found. The most useful ones seem to be magnetic Wannier states, which are localized in the two directions perpendicular to the magnetic field. We found that the ground state described in such a way embraces, for low fields, a large number of adjacent quantum wells, and is localized in the transverse direction on a distance of the order of $2\pi(a_0^2/d)$, where a_0 is the magnetic length and d the superlattice period. We studied the influence of interface disorder on the conduction states, and found that the magnetotunneling experiments[5] show that the conduction wave functions are coherent, at least on a distance of more than 400 Å (eight successive quantum wells).

These results were generalized to the case of valence states. We first modeled the superlattice dispersion curves in the absence of magnetic field by combining longitudinal tight-binding and transverse $\mathbf{k}\cdot\mathbf{p}$ techniques. This provided, with a minimum of computations, the superlattice dispersion curves which account for the coupling between heavy and light holes. The valence Landau-level structure was then easily found using the same magnetic translation arguments. Due to the interaction between heavy and light holes, the Landau-level energies do not vary linearly with the field. The high-index Landau-level structure appeared extremely complex, but was qualitatively understood as coming from the accumulation of anticrossings between two fan diagrams associated with the first heavy- and light-hole subbands.

Finally, we think our model of the SL valence states should be useful for calculating the excitonic states, and perhaps also the magnetoexciton, in short-period superlattices, without leading to overly cumbersome computations (all the numerical calculations we performed in this paper were implemented on a personal computer).

ACKNOWLEDGMENTS

The author is grateful to J.C. Maan and A. Fasolino for fruitful discussions on magnetotunneling in superlattices, and to J.Y. Marzin, J.M. Gérard, K. Elcess, and R. Padjen for their advice and comments on this work.

[1]J. F. Palmier, H. Le Person, C. Minot, and A. Sibille, J. Phys. (Paris), Colloq. **48**, C5-443 (1987).
[2]A. Chomette, B. Devaud, R. Regreny, and G. Bastard, Phys. Rev. Lett. **57**, 1464 (1986).
[3]E. E. Mendez, F. Agullo-Rueda, and J. M. Hong, Phys. Rev. Lett. **60**, 2426 (1988).
[4]P. Voison, J. Bleuse, C. Bouche, S. Gaillard, C. Alibert, and A. Regreny, Phys. Rev. Lett. **61**, 1639 (1988).
[5]G. Belle, J. C. Maan, and G. Weimann, Solid State Commun. **56**, 65 (1985).
[6]T. Duffield, R. Bhat, M. M. Koza, D. M. Hwang, P. Grabbe, and S. J. Allen, Jr., Phys. Rev. Lett. **56**, 2724 (1986).
[7]J. C. Maan, in *Festkörperprobleme (Advances in Solid State Physics)*, edited by P. Grosse (Vieweg, Braunschweig, 1987), Vol. 27, p. 137, and references therein.
[8]A. Fasolino and M. Altarelli, in *Band Structure Engineering in Semiconductors Microstructures*, edited by R. A. Abram and M. Jaros (Plenum, New York, in press).
[9]R. Peierls, Z. Phys. **80**, 763 (1983).
[10]E. Brown, Phys. Rev. **133**, 1038 (1964).
[11]J. Zak, Phys. Rev. **134**, 1602 (1964).
[12]G. H. Wannier, Rev. Mod. Phys. **34**, 645 (1962).
[13]W. Kohn, Phys. Rev. **115**, 1460 (1959).
[14]G. Bastard and J. A. Brum, IEEE J. Quantum Electron. **QE-22**, 1625 (1986).
[15]J. B. Gibson, Bull. Am. Phys. Soc. **3**, 146 (1958).
[16]G. Bastard, Acta Electron. **25**, 147 (1983).
[17]See, for instance, C. Itzykson and J. B. Zuber, *Quantum Field Theory, International Series in Pure and Applied Physics* (McGraw-Hill, New York, 1980).
[18]T. Ando, J. Phys. Soc. Jpn. **39**, 411 (1975).
[19]R. Altarelli and G. Platero, Surf. Sci. **196**, 540 (1988).
[20]E. A. Johnson, A. MacKinnon, and C. J. Goebel, J. Phys. C **20**, L521 (1987).
[21]D. Paquet, Superlatt. Microstruct. **2**, 429 (1986).
[22]J. M. Luttinger, Phys. Rev. **102**, 1030 (1956).
[23]M. Altarelli, U. Ekenberg, and A. Fasolino, Phys. Rev. B **32**, 5138 (1985).
[24]T. Ando, J. Phys. Soc. Jpn. **54**, 1528 (1985).
[25]A. Fasolino and M. M. Altarelli, in Proceedings of the 19th International Conference on the Physics of Semiconductors, Warsaw, 1988 (unpublished).